79-4021

Prediction of a Three-Dimensional Circular Turbulent Jet in Crossflow

D. Adler* and A. Baron†
Technion, Israel Institute of Technology, Haifa, Israel

A quasi-three-dimensional integral method is used to solve the problem of the isothermal incompressible turbulent jet. The jet is submerged and is circular at its origin. The mathematical model is based on two integral momentum equations, one written for a direction parallel to the jet centerline and the other for a direction perpendicular to the centerline. For their solution, the entrainment rate into the jet is determined as the linear combination of a modified straight jet entrainment and the entrainment into a vortex pair. The family of velocity profiles required for the integration of the momentum equations is three-dimensional. The profiles are determined along the jet centerline on the basis of the distorted jet cross sections, thus being nonsimilar. The mathematical model is numerically solved, yielding the internal jet flowfield. Results are compared to experiments with different injection velocity to crossflow velocity ratios and with different injection angles. Agreement between theory and experiment is found to be satisfactory in some cases and good in others.

Nomenclature

A = cross-section area
A_0 = initial cross-section area
A_1 = constant in Eq. (8)
b = jet width in the ξ direction
C_D = drag coefficient
D_0 = initial jet diameter
E = entrainment function [defined in Eq. (A2)]
F_c = centrifugal force
G = rate of increase of a straight jet radius [defined in Eq. (6)]
h = maximum jet velocity excess (defined in Fig. 1)
I_1 $\equiv \int_A U dA$
I_2 $\equiv \int_A U^2 dA$
K_1 = constant in Eq. (8)
K_2 = constant in Eq. (8)
L_p = length of potential core
M $\equiv U_0/W$
$\dot{m}$ = mass flux through A
$\dot{m}_0$ = initial mass flux through A_0
N = number of vortices [Eqs. (10-12)]
n = current number of a vortex [Eqs. (10-12)]
P = constant in Eq. (13)
p_{st} = static pressure
Q = constant in Eq. (13)
R = equivalent radius of the jet
R_0 = initial radius of a jet
R_p = radius of the potential core (defined in Fig. 3)
$\bar{R}$ $\equiv R/R_0$
T = auxiliary function
T_{max} = maximum value of the auxiliary function
U = normalized velocity in the jet in the Z direction
u = actual velocity in the jet in the Z direction, $u = W\cos\theta + Uh$ (see Fig. 1)
u_0 = initial jet velocity
V_ξ = induced velocity of a vortex in the ξ direction
V_η = induced velocity of a vortex in the η direction
W = velocity of the crossflow
X = coordinate in Fig. 1
Y = coordinate in Fig. 1
Z = coordinate in the direction of the centerline (defined in Fig. 1)
Z_s = coordinate in the direction of the centerline in a straight jet
$\bar{Z}_p$ = dimensionless distance along the centerline of a developing vortex pair, $\bar{Z}_p \equiv (Z/R_0)$
α = constant in Eq. (8)
Γ_0 = constant defined in Eq. (12)
η = coordinate defined in Fig. 1
θ = angle defined in Fig. 1
ν_t = turbulent dynamic viscosity
ξ = coordinate perpendicular to η in Fig. 1
ρ = density

Received June 2, 1978; revision received Sept. 19, 1978.

Index category: Jets, Wakes, and Viscid-Inviscid Flow Interactions.

*Associate Professor, Faculty of Mechanical Engineering.
†Research Associate, Faculty of Mechanical Engineering.

Introduction

THE turbulent mixing of a circular jet in crossflow is of significant importance in combustion engineering, VTOL or STOL aircraft design, heat transfer calculation of injection cooled gas turbine blades, missile control system development, and environmental engineering. Because of its practical importance, this mixing problem received much attention, and many attempts, theoretical as well as experimental, were made to throw some light on this extremely complex flow problem.

A number of approximate predictive methods have been developed in the literature.[1-8] All these are basically integral methods based on simplifying assumptions, introduced for mathematical simplicity. Thus, simple similarity profiles (approximately true only for a straight jet) are used, or the complex jet cross-section geometry, perpendicular to the centerline, is represented by rectangles, circles, or ellipses. These approximate approaches are well justified because a solution of the Reynolds equation in this turbulent mixing field seems to be an enormous task if only the prediction of the "turbulent viscosity" is considered (not to mention entrainment or numerical problems). Simple mixing length or kinetic energy-dissipation rate concepts cannot represent reality because of strong and not negligible curvature effects,[9-13] and coriolis-like, centripetal acceleration field effects.[14-16]

One of the unknowns in integral mixing field prediction methods is usually the shape of jet cross section. In this connection, Braun and McAllister,[17] Margason,[18] and Hackett and Miller[19] all mention Chen's idea[20] of vortices distributed along the edge of the orifice in potential flow. This idea was further improved by Strauber[21] at a later time. Resuling cross-section shapes were close to reality. However, the idea was not extended to full jet mixing calculation; rather, it was concentrated merely on cross-section prediction.

The second unknown in integral methods is a velocity profile parameter(s). Such a parameter is usually connected to an appropriate similarity assumption, which actually does not exist in a curved jet. Therefore, Keffer and Baines[3] divided the jet into three similarity regions: potential core, developed turbulent flow, and far downstream region. They assumed that the main cross-section distortion happens in the potential core region, but Kamotani and Greber's measurements[23] show that this is not accurate. Kamotani and Greber further conclude that similarity cannot exist in a curved jet. This conclusion is obvious from theoretical considerations.

The problems of similarity and cross-section shape in the curved jet are closely associated with entrainment. An entrainment sub model coupled to velocity decay and cross-section shape and growth is required for a solution. In Refs. 4, 5, 7, and 24 the entrainment is calculated on the basis of the velocity difference between the jet and its surroundings. In the models reported in Refs. 1, 2, and 6 the entrainment is represented in a similar way by the cross-section growth and is determined with the continuity equation. Baines and Keffer[3,25] go a step further and assume that entrainment is composed of two components—straight jet entrainment and helical entrainment. Schwartz and Tulin[26,27] suggest that the local jet growth can be represented by a vortex pair. Their idea is used here.

The present method was developed with the aim of improving the integral method and extending its ability to predict the inner structure of the deflected jet more accurately; or, in other words, to include nonsimilar three-dimensional effects. Modifications included in the method are: 1) improved jet growth function is based on straight jet growth and the vortex pair concept; 2) cross-section shape is not of an assumed simple geometry but is calculated approximately, resulting in a more realistic horseshoe shape; 3) velocity profiles are nonsimilar quasi-three-dimensional. They are not similarity profiles because their definition is based on the distorted shape of the jet cross section.

Mathematical Model

The model is developed on the basis of some simplifying assumptions, namely: 1) external flowfield is irrotational; 2) the mixing field is isothermal and of uniform composition (no heat transfer or diffusion); 3) the flow is turbulent; 4) the flow is incompressible and steady; 5) the jet centerline is defined as the locus of the momentum centers of cross sections; 6) velocities are parallel to the centerline; 7) cross-section boundary of the jet is the locus of points at which the velocity excess in the direction of the centerline vanishes (or is smaller than a prescribed small value); 8) pressure on cross sections is uniform and proportional to $W\cos\theta$; 9) most of the entrainment takes place in the vortex pair tail.

A control volume in the jet is defined in Fig. 1. It is used to derive the governing two momentum equations of the integral model. These two integral momentum equations, together with four additional equations—i.e., the expansion rate equation, the shape equations, and the normalized velocity profile equation—describe the jet mixing field completely.

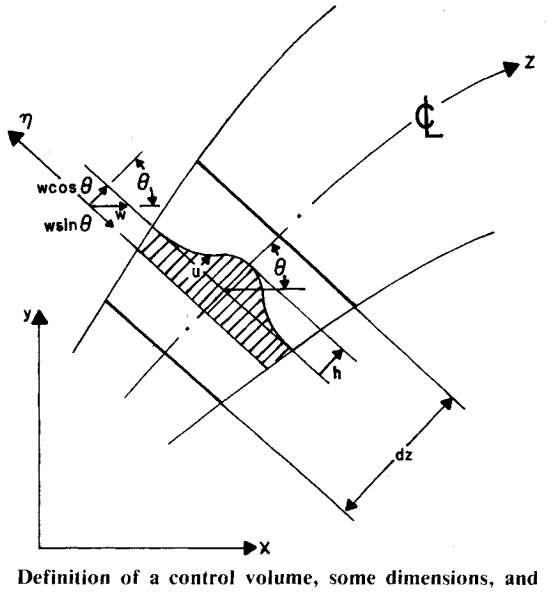

Fig. 1 Definition of a control volume, some dimensions, and the coordinate systems used to analyze the deflected jet.

A. Momentum Equation in Centerline Direction

For steady flow, surface forces are equated to momentum flux, and gravity is neglected. The result is

$$A\frac{dp_{st}}{dZ}+\frac{d}{dZ}\int_A \rho u^2 dA=\rho EW\cos\theta \tag{1}$$

In view of assumptions 8 and 1 using Euler's equation for the external flow, we can write

$$\frac{A}{\rho}\frac{dp_{st}}{dZ}=\frac{I}{2}AW^2\sin\theta\cos\theta\frac{d\theta}{dZ} \tag{2}$$

Furthermore, the volumetric entrainment rate E is given in Eq. (A3) of the Appendix.

With Eqs. (2) and (A3), the rearranged form of Eq. (1) will be

$$\frac{dh}{dZ}=\frac{W^2A\frac{d\theta}{dZ}\sin 2\theta-\frac{dI_2}{dZ}h^2-Wh\left(\frac{dI_1}{dZ}\cos\theta-\frac{d\theta}{dZ}2I_1\sin\theta\right)}{2I_2h+I_1W\cos\theta} \tag{3}$$

B. Momentum Equation in Direction Normal to the Centerline

Here surface forces and centrifugal body forces are equated to the momentum flux due to entrainment. Surface forces are calculated as a "drag force" acting on the jet considered to be "rigid." A drag coefficient C_D (having values similar to C_D of a circular cylinder) is utilized for this purpose, and the force can be expressed as $C_D(b/2)\rho W^2\sin^2\theta dZ$. The centrifugal force is

$$F_C=\rho[I_2h^2+2I_1hW\cos\theta+AW^2\cos^2\theta](d\theta/dZ)dZ \tag{4}$$

The η momentum flux is $\rho EW\sin\theta dZ$ and E is given in Eq. (A3). Using these expressions, the η momentum equation is given the following form:

$$d\theta/dZ=\frac{\frac{I}{2}C_DbW^2\sin^2\theta+W\sin\theta\left(h\frac{dI_1}{dZ}+I_1\frac{dh}{dZ}\right)+W^2\sin\theta\cos\theta\frac{dA}{dZ}}{AW^2\sin^2\theta-h^2I_2-2hI_1W\cos\theta-AW^2\cos^2\theta} \tag{5}$$

To complete the formulation the rate of the jet growth, the shape of the cross sections, and the velocity profiles have to be determined.

C. Expansion Rate of the Jet Cross-Section Area

It is assumed here that the jet cross-section area growth is a linear superposition of two growing mechanisms: 1) growth of a straight turbulent jet in a quiescent environment; and 2) growth of a vortex pair (in accordance with assumption 9). Although this model of jet growth seems to be an oversimplification, it yields acceptable results, as will be seen later in comparison to experiments.

For the straight jet growth in quiescent environment we assume

$$dR/dZ_S = G \tag{6}$$

Abramovich[1] suggests that $G=0.22$ for turbulent jets, and we will use this value in the present study. Equation (6), written for a straight jet, is modified for a curved jet to give

$$\frac{dR}{dZ} = \frac{Gh}{h+W\cos\theta} \tag{7}$$

The growth of a vortex pair was studied by Tulin and Schwartz.[26,27] They suggested a growth rate of

$$\frac{1}{\alpha}\frac{d\bar{R}}{d\bar{Z}_p} = \left(K_1 - \frac{K_2}{\alpha}\frac{d\bar{R}}{d\bar{Z}_p}\right)\bar{R}^{(1-A_1)} \tag{8}$$

Tulin and Schwartz achieved good agreement with experiments using $\alpha K_1 = 0.38$ and $K_2 = 0.5$. A_1 is a measure to the cancellation of vorticity in the vortex pair tail. For $A_1 = 0$, cancellation is complete. In the present case, due to the sweeping effect of the crossflow, cancellation is not complete; therefore, $A_1 > 0$. A value of $A_1 = \exp[-2ZW\sin\theta_0/\pi D_0 u_0](M/6.2)$ gave good results, though the generality of this expression is not completely verified.

Equation (8), modified for curved jet conditions, is added to Eq. (7) to yield the jet growth written in terms of cross-section area A, rather than in terms of equivalent normalized radius $\bar{R}$.

$$\frac{dA}{dZ} = \frac{2\sqrt{\pi A}}{h+W\cos\theta}\left[Gh + \frac{\alpha K_1 W\sin\theta}{(A_0/A)^{(1-A_1)/2}+K_2}\right] \tag{9}$$

This equation, with $W=0$, reduces to $dR/dZ_S = G$. Indeed, for $W=0$ the expression for a straight jet in quiescent environment is expected.

D. Cross-Section Shape

The aim of the cross-section shape calculation is to predict approximately the development of the geometry (but not the areas) of these shapes from a circle into the developed horseshoe configuration. This shape development contains much of the nonsimilarity of the mixing process, so that its prediction is essential for a representative model. Chen[20] and Strauber[21] studied the deformation of a potential circular jet deflected by crosswind. The cross-section distortion is determined by evenly seeding a finite number N of vortices on the instantaneous boundary of the jet and calculating their displacement over a small time period dt due to their induced velocity. The induced velocities of the vortices including viscous damping are given by the following three equations. The detailed derivation of these equations is described in Refs. 20 and 21.

$$V_\eta = \frac{2\Gamma_0}{\pi}\sum_{n=1}^{N}\sin\left[\frac{2\pi}{N}(n-1)\right] \times \frac{(\xi-\xi_n)\left\{1-\exp\left[\dfrac{(\eta-\eta_n)^2+(\xi-\xi_n)^2}{4\nu_t}\right]\right\}}{(\eta-\eta_n)^2+(\xi-\xi_n)^2} \tag{10}$$

$$V_\xi = -\frac{2\Gamma_0}{\pi}\sum_{n=1}^{N}\sin\left[\frac{2}{N}(n-1)\right] \times \frac{(\eta-\eta_n)\left\{1-\exp\left[\dfrac{(\eta-\eta_n)^2+(\xi-\xi_n)^2}{4\nu_t}\right]\right\}}{(\eta-\eta_n)^2+(\xi-\xi_n)^2} \tag{11}$$

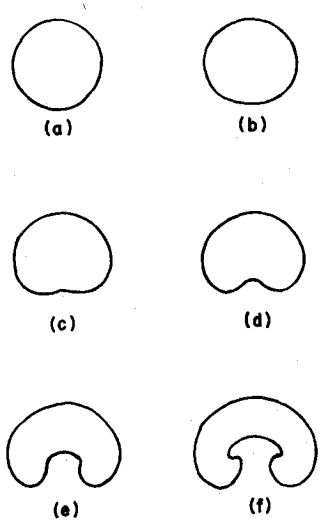

Fig. 2 Development of jet cross sections downstream along its centerline.

where

$$\Gamma_0 = W\sin(\theta)R_0\sin(\pi/N) = \text{const.} \tag{12}$$

For a known instantaneous cross section, the induced velocity components V_x and V_y of each vortex are calculated. The vortex is then displaced by $V_x dt$ and $V_y dt$. All the new positions of the vortices describe the new cross-section shape. The viscosity ν_t for the turbulent jet can be calculated with Owen's formula.[22] Figure 2 gives an example of computer plotted results of such a computation.

E. Normalized Velocity Distribution

As the curved jet is not a similarity phenomenon, similarity profiles cannot be used in the present integral method if it is to be realistic. Furthermore, the profiles should be three-dimensional to represent the flow correctly. However, in an integral method, only parameters of a profile family, not exact profiles, are determined. Therefore, a special, downstream varying, calculated family of velocity profiles is used. In the nonnormalized form, they include the familiar parameter h, but they are not similarity profiles because they are calcuated on the basis of the varying cross-section shape as determined by Eqs. (10) and (11). This family of velocity profiles, in analogy to similarity profiles in classical integral methods, has to contain qualitatively correct velocity profiles that also satisfy the physical boundary conditions. Therefore, to satisfy these two simple conditions, and these two conditions only, the family of velocity profiles U is computed using the previously determined cross-section shapes and an auxiliary function T, which is numerically computed. T satisfies $\nabla^2 T = q$ inside the domain of the cross section (q being a constant in the domain) and $T=0$ on the boundary. With T known, U is given by

$$U = \left(\frac{T}{T_{\max}}\right)^{\frac{T}{T_{\max}}(P-Q)+Q+1} \tag{13}$$

where Q and P are distortion parameters used to adjust the profiles to correspond to measured turbulent velocity profiles. Q distorts the function in the neighborhood of the boundaries of the domain while P affects the profile inside the domain, as shown in Fig. 3. These parameters were evaluated using

$$P = 0.15 + \frac{0.126(Z-L_p)}{15D_0 - L_p}, \quad Q = 0.945$$

which gave good results in the present examples though their generality is not confirmed. The value of the constant q is immaterial because the normalized function $T/T_{\max}$ is used to

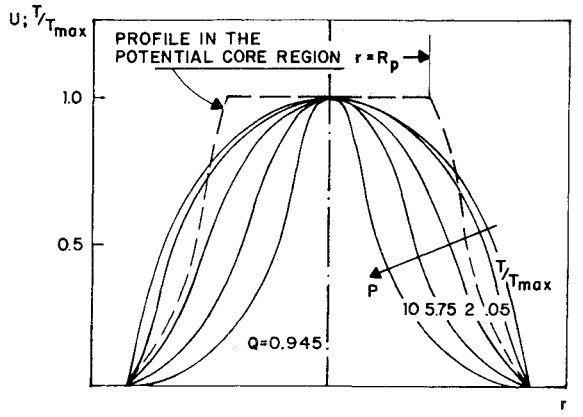

Fig. 3 Normalized velocity profiles as used in the integral solution (in this case for a circular cross section).

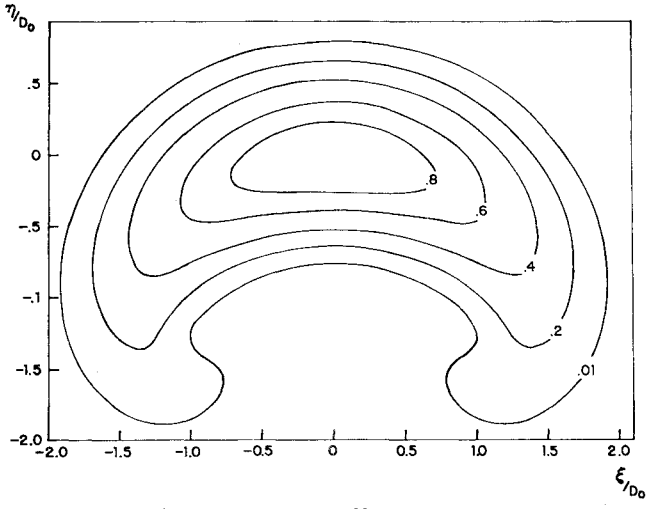

Fig. 4 Lines of constant velocity U in a typical horseshoe cross section.

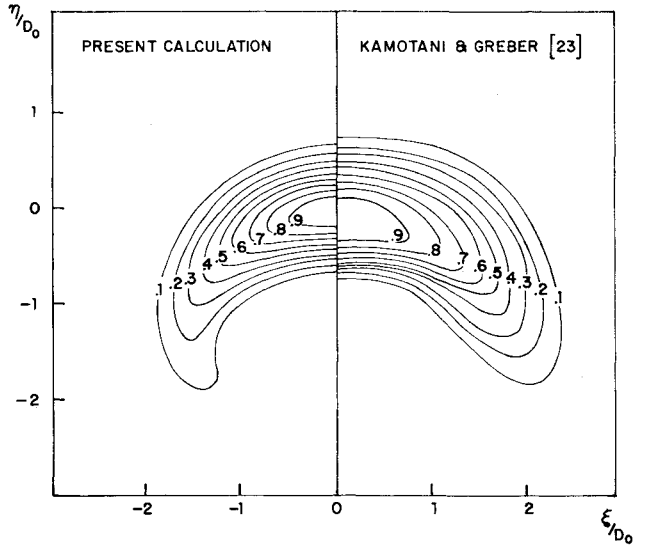

Fig. 5 Comparison of cross sections and U = const. lines for $M = 3.91$ and at $Z/D_0 = 7$ ($\theta_0 = 90$ deg).

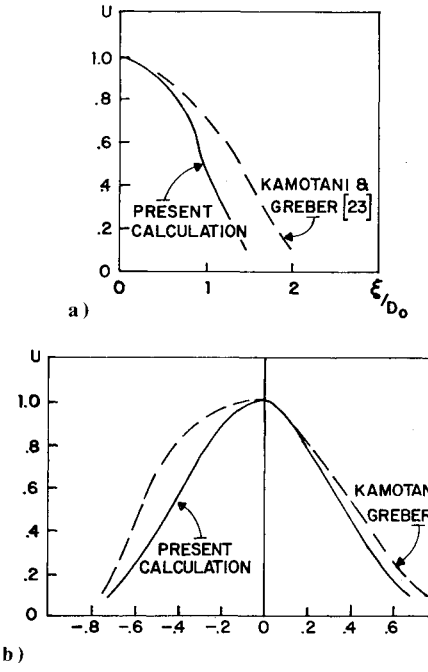

Fig. 6 Comparison of velocity profiles in Fig. 6: a) along $\eta/D_0 = 0$, b) along $\xi/D_0 = 0$.

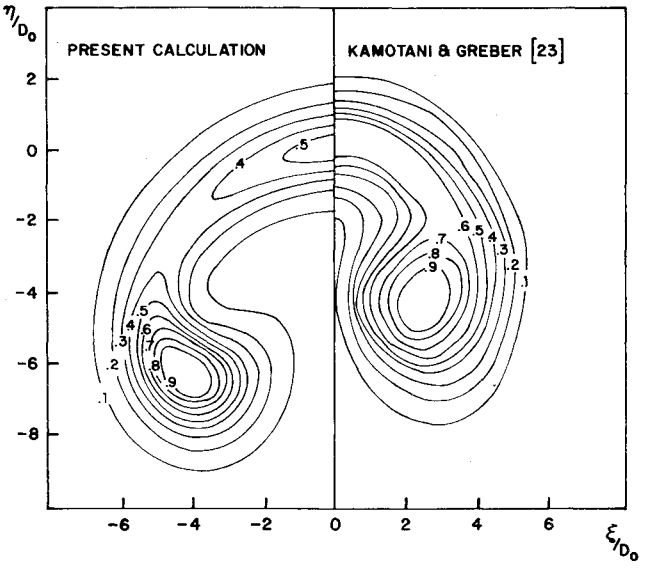

Fig. 7 Comparison of cross sections and U = const. lines for $M = 7.73$ and at $Z/D_0 = 23$ ($\theta_0 = 90$ deg).

determine U. $q = 1$ was used in the present work. Physically, the curved jet can be divided into three major regions: 1) the potential core region, where the excess centerline velocity is constant; 2) the deflection region, where the flow is highly nonsimilar; and 3) the similarity region far downstream, where the jet is almost parallel to the deflecting main flow.

Expression (13) can also be used to describe the profile in the potential core region by cutting U at $r = R_p$ and renormalizing the profile so that $U = 1$ on the centerline. Such a potential core profile is shown in Fig. 3 as a broken line. Figure 4 gives an example of a computer-plotted velocity distribution in the deflection region.

The curved jet is described by Eqs. (3) (5), and (9) together with cross-section shapes according to Eqs. (10) and (11) and velocity distributions given by Eq. (13). Equations (3), (5), and (9) are ordinary coupled differential equations. They are numerically solved with a combined four point Runge-Kutta procedure for the unknown functions h, A, and θ in terms of the independent variable Z. The functions I_1, I_2, and b required for this solution are obtained in each Runge-Kutta step with the results of Eq. (13) numerically integrated over the appropriate cross-section area. The shapes of these cross sections are determined by Eqs. (10) and (11) and are subsequently corrected (maintaining geometric similarity) to

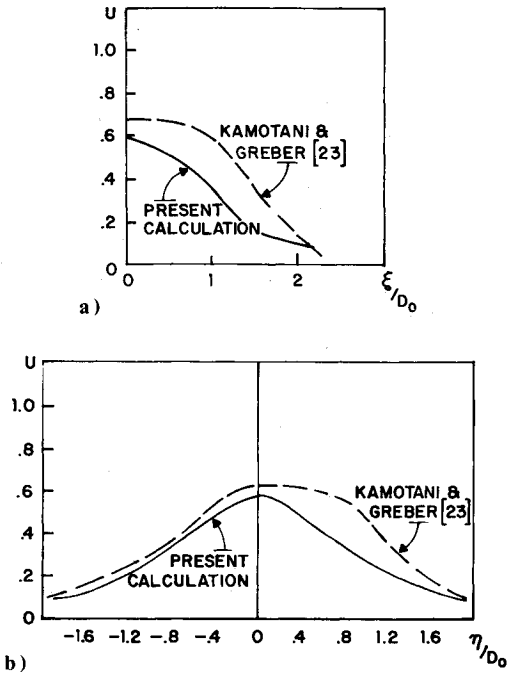

Fig. 8 Comparison of velocity profiles in Fig. 7: a) along $\eta/D_0 = 0$, b) along $\xi/D_0 = 0$.

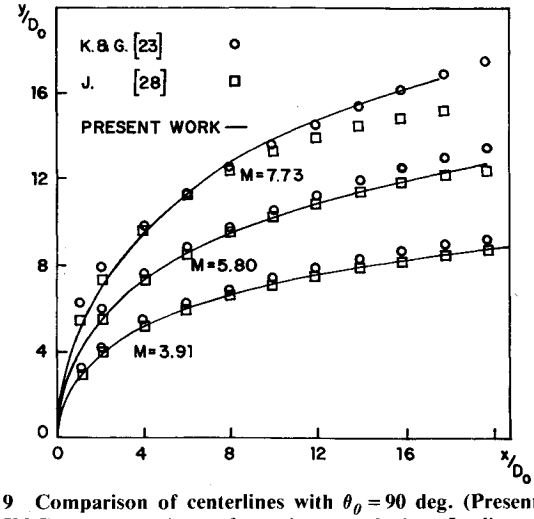

Fig. 9 Comparison of centerlines with $\theta_0 = 90$ deg. (Present work and K&G are centerlines of maximum velocity. Jordinson's are centerlines of maximum total pressure for M values of 8.1, 6.2, and 4.3).

include the area as predicted by Eq. (9). The time intervals Δt, required for vortices displacement calculation, are calculated with $\Delta t = \Delta Z/\bar{u}$, where $\bar{u}$ is the average jet velocity and ΔZ is the Runge-Kutta step.

In the potential core region and the similarity region the equations can be simplified. The centerline velocity in the potential core region is simply given by

$$h = u_0 - W\cos\theta \tag{14}$$

which is used instead of Eq. (3). The length of the potential core is derived using the empirical correlations of Kamotani and Greber.[23]

$$L_p = D_0/(0.154 + 0.72M) \tag{15}$$

Once the length of the conical core L_p is known, the values R_p required for the velocity profiles are determined easily. In the similarity region, the cross-section shape and profile

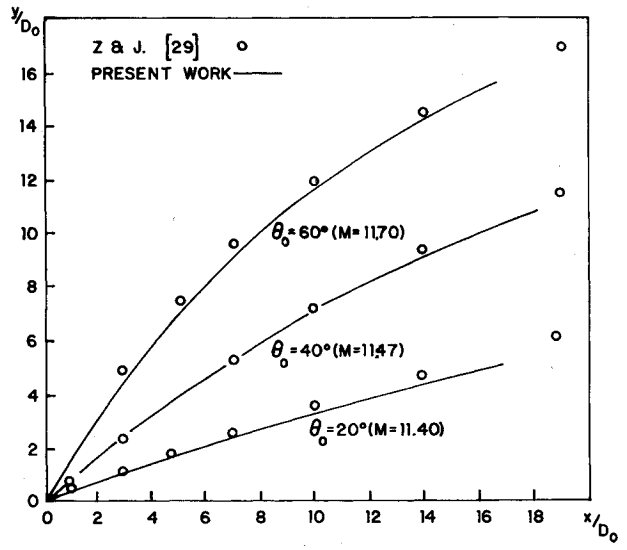

Fig. 10 Comparison of maximum velocity centerlines of jets injected in the direction of the cross flow ($\theta_0 < 90$ deg).

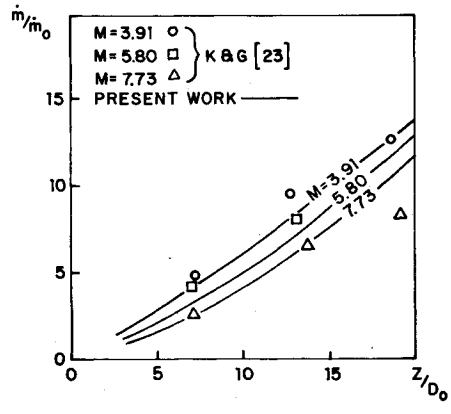

Fig. 11 Comparison of the relative mass flux for jets with $\theta_0 = 90$ deg.

calculations are not necessary. Instead, similarity of shapes and profiles is used to determine the values of I_1, I_2, and their derivatives to be used in the solution of Eqs. (3), (5), and (9).

Comparison Between Calculated Results and Experiments

The present mathematical model was solved numerically for a number of jets for which experimental data are available in the literature. The experiments chosen ranged from M values of about 4 to 12, from Z/D_0 values of about 0 to 25 (in some cases well into the similarity region), and from injection angles of 90 to 20 deg, so that the present method is tested over a reasonably wide field of jet parameters.

Figure 5 compares velocity contours measured by Kamotani and Greber[23] at $\theta_0 = 90$ deg to results of the present method for a case where the velocity maximum is located on the centerline. Figure 6 shows velocity profiles along the axes of Fig. 5. Figure 7 describes another experiment of Kamotani and Greber[23] with $\theta_0 = 90$ deg at larger M values and further downstream, where the velocity maximum is not located on the centerline but rather in the centers of the horseshoe branches. Figure 8 shows velocity profiles along the axes of Fig. 7. Here agreement is not as good as in the previous case, but the general character of the jet (i.e., the two velocity peaks) is well predicted by the present method.

In Fig. 9 calculated centerlines for $\theta_0 = 90$ deg are compared for three M values with experiments of Kamotani and Greber[23] and Jordinson.[28] In Fig. 10 calculated centerlines

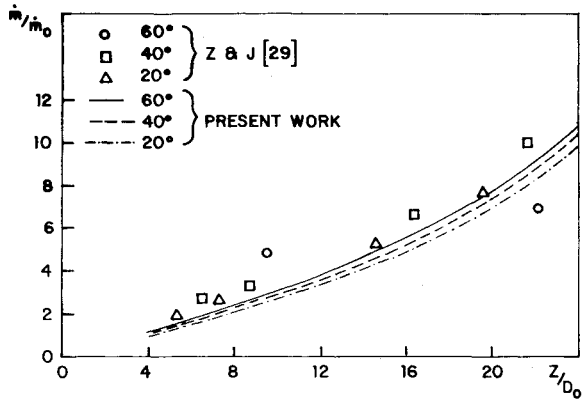

Fig. 12 Comparison of the relative mass flux for jets with $\theta_0 < 90$ deg (M values as in Fig. 10).

for three θ_0 values and a constant higher M value are compared to Zandbergen and Joosen's experiments.[29] Agreement between prediction and experiment is good over the whole range of jet injection angles and M values.

The calculated relative mass flux $\dot{m}/\dot{m}_0$, which is a measure of entrainment as represented by the jet growth model and the velocity profiles, is compared to experiments of Kamotani and Greber[23] for $\theta_0 = 90$ deg injections in Fig. 11 and to Zandbergen and Joosen[26] for a higher M value and lower injection angles in Fig. 12. Here scatter is bigger because of the difficulty in the jet boundary definition. The ratio $\dot{m}/\dot{m}_0$ for constant density is calculated with

$$\dot{m}/\dot{m}_0 = [\int_A (hU + W\cos\theta)\,dA]/u_0 A_0 \qquad (16)$$

$u_0 A_0$ is well defined, while definition of A, the integration boundary of the nominator, is not exact at the jet edge, the region where u gradients are small. The end result of the integration depends on A because external velocity is not zero.

Conclusions

An integral method using a new family of nonsimilar quasi-three-dimensional velocity profiles (based on a realistic jet cross-section shape), and a new jet growth model (based on a linear combination of straight jet and vortex pair entrainments) is developed to describe the curved jet. It is demonstrated that this technique can predict in principle the nonsimilar three-dimensional mixing region of a jet in crossflow, including its internal velocity field. The constant q and the parameters P and Q as determined in the present work gave satisfactory agreement for $4 < M < 12$ and $20 \text{ deg} < \theta < 90$ deg. The accuracy of their use outside this range is not known and should be the subject of future investigations. More experiments are necessary to derive reliable correlations for these coefficients in order to increase the accuracy and, much more important, the generality of the method. In the meantime, however, the technique can be used in the range of jet parameters tested for incompressible isothermal submerged jets in crossflows. Another problem is the applicability of the present method in cases where $\theta > 90$ deg (injection against the crossflow). In this case some of the present assumptions concerning rate of entrainment and cross-section shape might not be acceptable. Extension of the technique to compressible nonisothermal deflected jets is possible and will be carried out in the near future.

Appendix—Derivation of the Entrainment Rate Equation for Incompressible Jets

The control volume of Fig. 1 is used for this derivation. The mass flux through a jet cross section, A, is

$$\rho\int_A u\,dA = \rho\int_A (Uh + W\cos\theta)\,dA = \rho I_1 h + \rho A W\cos\theta \qquad (A1)$$

The volumetric entrainment rate is defined as

$$E \equiv \frac{I}{\rho}\frac{d}{dZ}(\rho I_1 h + \rho A W\cos\theta) \qquad (A2)$$

and differentiation gives

$$E = \frac{d}{dZ}(hI_1) + W\frac{d}{dZ}(A\cos\theta) \qquad (A3)$$

Acknowledgment

This article is the result of A. Baron's MSc. thesis, supervised by D. Adler.

References

[1] Abramovich, G. N., *The Theory of Turbulent Jets*, MIT Press, Cambridge, Mass., 1963.

[2] McAllister, J. D., "A Momentum Theory for the Effects of Cross Flow on Incompressible Turbulent Jets," Ph.D. Thesis, The Univ. of Tennessee, 1968.

[3] Keffer, J. F. and Baines, W. D., "The Round Turbulent Jet in a Cross-Wind," *Journal of Fluid Mechanics*, Vol. 15, April 1963, pp. 481-496.

[4] Snel, H., "A Model for the Calculation of the Properties of a Jet in a Cross Flow," NLR TR 74080 U., Netherland Nationaal Lucht En Ruimtevaart-Laboratorium, Amsterdam, Netherlands, 1974.

[5] Stoy, R. L. and Ben Haim, Y., "Turbulent Jets in a Confined Cross Flow," *Journal of Fluids Engineering*, Vol. 95, Dec. 1973, pp. 551-556.

[6] Sucec, J. and Bowley, W. W., "Prediction of the Trajectory of a Turbulent Jet Injection into a Cross Flowing Stream," *Journal of Fluids Engineering*, Vol. 98, Dec. 1976, pp. 667-673.

[7] Clamp, B., G., "Smoke Abatement in Coal Field Metallurgical Furnaces," Ph.D. Thesis, University of Sheffield, England, 1959.

[8] Wooler, P. T., "Development of Analytical Model for the Flow of a Jet into a Subsonic Cross-Wind," NASA SP-218, Sept. 1969.

[9] Bradshaw, P., "The Analogy Between Streamline Curvature and Buoyancy in Turbulent Shear Flow," *Journal of Fluid Mechanics*, Vol. 36, March 1969, pp. 177-191.

[10] Bradshaw, P., "Complex Turbulent Flows," *Journal of Fluids Engineering*, Vol. 96, June 1975, pp. 146-154.

[11] So, R.M.C. and Mellor, G. L., "Experiments on Convex Curvature Effects in Turbulent Boundary Layers," *Journal of Fluid Mechanics*, Vol. 60, Aug. 1973, pp. 43-62.

[12] So, R.M.C. and Mellor, G. L., "Experiment on Turbulent Boundary Layers in a Concave Wall," *Aeronautical Quarterly*, Vol. 26, Feb. 1975, pp. 35-40.

[13] Ramaprian, B. R. and Shivaprasad, B. G., "The Structure of Turbulent Boundary Layers along Mildly Curved Surfaces," *Journal of Fluid Mechanics*, Vol. 85, March 1978, pp. 273-303.

[14] Johnston, J. P., "The Suppression of Shear Layer Turbulence in Rotating Systems," *Journal of Fluids Engineering*, Vol. 95, June 1973, pp. 229-236.

[15] Johnston, J. P. and Eide, S. A., "Turbulent Boundary Layers on Centrifugal Blades: Prediction of the Effects of Surface Curvature and Rotation," *Journal of Fluids Engineering*, Vol. 98, Sept. 1976, pp. 374-381.

[16] Koyama, H., Masuda, S., Ariga, I., and Watanabe, I., "Stabilizing and Destabilizing Effects on Criolis Force on Two Dimensional Laminar and Turbulent Boundary Layers," ASME Paper 78-Gt-1, International Gas Turbine Conference, London, England, April 1978.

[17] Braun, G. W. and McAllister, J. D., "Cross Wind Effects on Trajectory and Cross Sections of Turbulent Jets," NASA SP-218, Sept. 1969.

[18] Margason, R. J., "Analytic Description of Jet-Wake Cross Sections for a Jet Normal to a Subsonic Free Stream," NASA SP-218, Sept. 1969.

[19] Hackett, J. E. and Miller, H. R., "The Aerodynamics of the Lifting Jet in a Cross Flowing Stream," NASA SP-218, Sept. 1969.

[20] Chen, C.L.H., "Aufrollung Eines Zylindrischen Strahles Durch Querwind," Doctoral Dissertation, Univ. of Gottingen, Gottingen, W. Germany, 1942,

[21] Strauber, M., "Berechnung von Strahlkonturen mit Hilfe eines Wirbelringmodells," *Zeitschrift fur Flugwissenschaften*, Vol. 23, Nov. 1975, pp. 394-400.

[22]Owen, P. R., "The Decay of a Turbulent Trailing Vortex," *Aeronautical Quarterly*, Vol. 21, Feb. 1970, pp. 69-78.

[23]Kamotani, Y. and Greber, I., "Experiments on a Turbulent Jet in a Cross Flow," NASA CR-72893 FTAS/TR-71-62, June 1971.

[24]Wooler, P. T., Burghart, G. H., and Gallagher, J. T., "Pressure Distribution on a Rectangular Wing with a Jet Exhausting Normally into an Airstream," *Journal of Aircraft*, Vol. 4, Nov.-Dec. 1967, pp. 537-543.

[25]Keffer, F. J., "The Physical Nature of the Subsonic Jet in Cross Stream," NASA SP-218, Sept. 1969.

[26]Tulin, M. P. and Shwartz, J., "The Motion of Turbulent Vortex Pairs in Homogeneous and Density Stratified Media," Tech. Rept. 231-15, Hydronautics, Inc., Laurel, Md., April 1971.

[27]Shwartz, J. and Tulin, M. P., "Chimney Plumes in Natural and Stable Surrounding," *Atmospheric Environment*, Vol. 6, Jan. 1972, pp. 19-35.

[28]Jordinson, R., "Flow in a Jet Directed Normal to the Wind," R&M No. 3074, British Aeronautical Research Council, 1956.

[29]Zandbergen, T. and Joosen, C.J.J., "Experimental Investigation of Round Turbulent Jet in a Cross Flow," NLR TR 74013, Nationaal Lucht En Ruimtevaart-Laboratorium, Amsterdam, Netherlands, 1973.